

Low-Cost Gradient Amplifiers for Small MRI Systems

Nathan Evetts and Mark S. Conradi

ABQMR, Inc.
2301 Yale Blvd SE, Suite C2
Albuquerque, NM 87106 USA

Prepared 24 August 2021 for submission to Journal of Magnetic Resonance
Revised October 26, 2021

Direct correspondence to either/both authors.

Emails:
nevetts@abqmr.com
msc@wuphys.wustl.edu

ABSTRACT

We describe low-cost gradient amplifiers for small MRI systems, such as those based on small/medium permanent magnets. The requirements for MRI gradient amplifiers are quite similar to those of modestly priced audio stereo power amplifiers. Such amplifiers for sound service can be modified to be DC coupled, extending their response down to zero frequency, as needed for MRI gradient service. We describe such modifications to one unit (Samson Servo 600) and mention a commercially available modification of another. The 600 is capable of an output greater than ± 8 A and ± 60 V, much greater than our needs for a greenhouse MRI. Audio amplifiers can be used this way as controlled voltage (CV) gradient amplifiers, with acceptable performance because the gradient coils typically have short L/R time constants. Superior performance can be had by using a controlled current (CC) "front end"; the circuit of our simple front end is included. The complete 3-axis CC system costs about \$1200.

INTRODUCTION

Gradient amplifiers are central and often expensive parts of MR imaging equipment. Much attention has been focused on powerful gradient amplifiers, addressing needs of clinical MRI [1-3]. For small-scale imagers, however, existing commercial gradient amplifiers have current and voltage capabilities much greater than needed. The absence of well-tailored solutions has compelled designers of such systems to build custom gradient amplifiers “from scratch” [4-8]. We set out to design high performance and inexpensive amplifiers by starting with slight modifications to commercially available audio power amplifiers, designed for sound service. This solution takes advantage of the low cost of consumer amplifiers and involves much less engineering work.

The requirements for good audio power amplifiers (“high fidelity”) are similar to those of gradient amplifiers. Generally, gradient service needs a frequency response extending up to perhaps 10 kHz, lower than the typical >50 kHz upper end of most audio amplifiers. The output power levels, requirements of linearity, and input voltage drive levels are all similar for these two applications. Because we operate at low resonance frequencies, we sought to avoid switching amplifier designs and their accompanying switching noise (e.g., high switching harmonics), instead staying with the older fashioned analog (class AB) amplifiers. Such analog audio units are available in power ratings (stereo) up to 600 W or more but they must be modified for DC coupling throughout to extend the response down to zero frequency.

In the realm of commercial gradient amplifiers, we have used and liked [9] AE Techron amplifiers [10]. Model 2105 is a ± 50 A, ± 150 V unit costing about \$6000 each (three are needed for three axis MRI). Compared to our needs (± 8 A and ± 35 V), this is vastly overpowered. In fact, our coils are passively cooled, so cannot tolerate large average power levels. The smaller model 7114 (maximum of ± 25 A, ± 40 V) costs less (about \$3500) but still is more than we need.

AMPLIFIER SOLUTIONS

A simple solution is to modify an audio unit for DC coupling and use it to directly drive the gradient coils. As a controlled voltage (CV) source with a low output impedance, the audio amplifier output voltage will be a faithful copy of the input voltage. However, the output *current* in the gradient coils will rise (and fall) with an exponential time constant of L/R in response to a step-waveform of the input voltage. Here L is the inductance and R the resistance of the gradient coil. For small imaging systems, this L/R time constant is often as small as 100 μ s, an acceptable level of performance, as long as the imaged spins do not have a very short T_2 . A second and real downside of CV operation is that the gradient

current will decrease as the gradient coils heat, due to a rising resistance of the copper coils. In the common approach of “shimming through the gradients”, even the shim currents will change slightly due to coil heating. But in many cases the overall results will be good, or good enough, if the gradient coils are not driven hard. One could add fixed power resistors in series with each gradient coil, so the total resistance R is larger (shorter time constant) and not so sensitive to average power put into the gradients. While this does seem inefficient, the simplicity is hard to beat.

We describe in the Appendix modifications needed for DC coupling to the Samson Servo 600 unit, selling for about \$350 for a 2-channel (stereo) device. We mention here that AE Techron offers conversion to DC coupling of the Crown XLi 800, a 2-channel audio (CV) unit of similar power output. The overall price from Techron of the amplifier converted to DC coupling is somewhat higher, of order \$1000. We note that we have used the Samson in CV and CC (controlled current) modes but have not tried the Techron-modified Crown XLi 800.

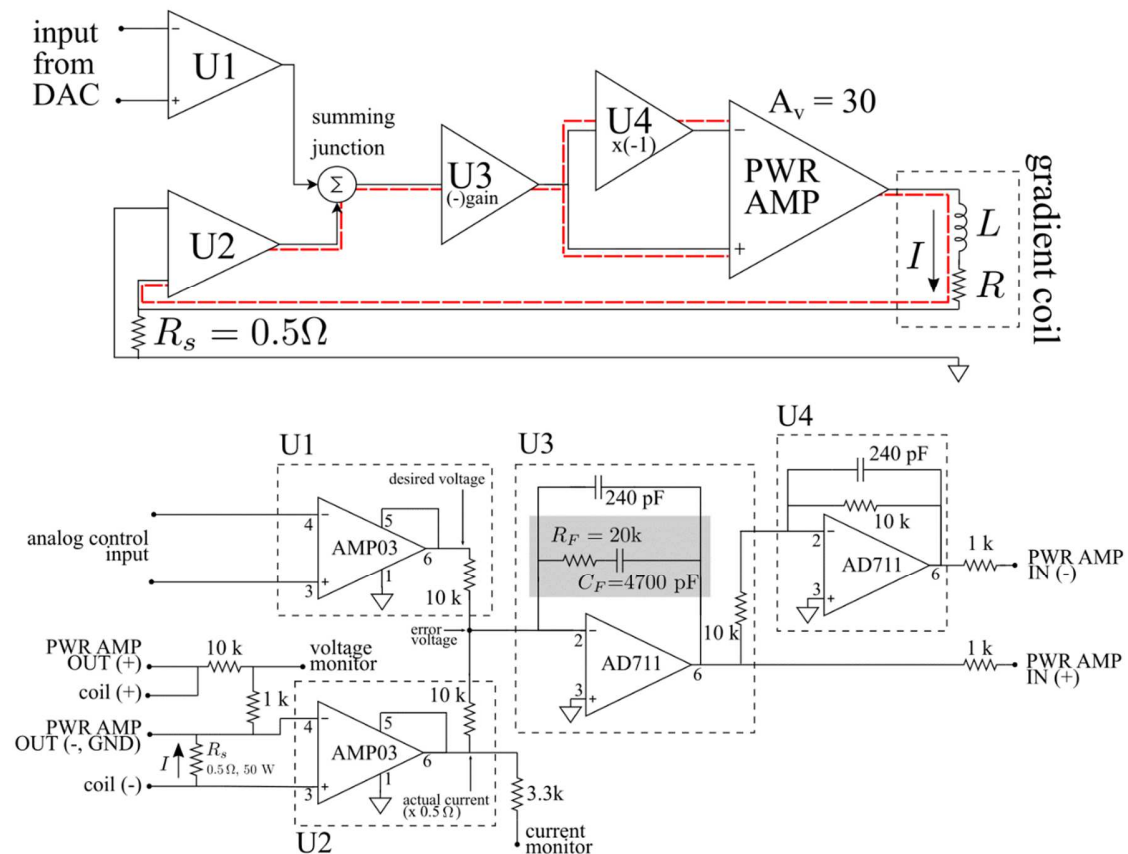


Figure 1: Block diagram (top) and circuit diagram (bottom) of the current controlled (CC) gradient amplifier. The red path (top) shows the overall feedback loop.

We built a simple 3-channel front end to convert our amplifiers to controlled current (CC) operation, a small construction project. The block and circuit diagrams (for a single channel) are shown in Figure 1. The $0.5\ \Omega$ current sensing power resistors, R_s , are in series with the return current (low side) from the gradient coils; the voltage across each resistor is strictly proportional to the gradient current. A unity-gain differential amplifier IC (U2) is used here. The voltage input from the DAC (digital to analog converter) of our Tecmag spectrometer, here a range of ± 10 volts, is applied to another unity-gain differential amplifier IC (U1). Consistent use of differential sensing reduces the 60 Hz hum in the system from power-line frequency ground currents and is highly recommended. The third IC (U3) combines the two signals to provide an error signal (essentially desired current minus actual gradient current); this error signal drives the input of the commercial audio power amplifier. A fourth IC (U4) makes an inverted copy of the error voltage, allowing a balanced differential drive to the audio amplifier. A voltage monitor port is formed from an 11:1 voltage divider (with an 11 k Ω impedance) in parallel with the power amplifier output. A current monitor port senses the output (current $\times 0.5\ \Omega$) of U2. These ports are useful diagnostics for a user attempting to debug a gradient or imaging system. The U3 and U4 IC outputs have 1 k Ω resistors in series with their outputs and small feedback capacitors that reduce their gains at the highest frequencies, to avoid oscillations resulting from the large loading capacitances of the audio standard TRS cables going to the Samson inputs.

Stability of negative feedback loops is a well-known issue. Essentially, to avoid self-oscillation at a high frequency, the overall loop gain must be below unity at any frequency where the net phase results in positive feedback through additional phase shifts of the components.

Thus, a key feature of the system is the R_F - C_F feedback (compensation) network around U3 (gray box, Figure 1). The gain of U3 is the ratio of this feedback network impedance to the 10 k Ω resistance from the output of U2. At low frequencies, the capacitive impedance of C_F dominates so U3 is an integrator. Thus, the overall gain around the feedback loop (see red loop in Figure 1) at DC is nearly infinite and any DC offset of the audio amplifier will be driven to zero. As in Figure 2, the gain of U3 varies as $1/\omega$ at low frequencies (ω) and becomes flat above $\omega = 1/(R_F C_F)$. The rest of the feedback loop has one major frequency dependence, that from the gradient coil's L and R; the audio amplifier itself is quite flat by comparison. This portion of the feedback loop's gain is flat at low frequencies and varies as $1/\omega$ above $\omega = R/L$ (again, see Figure 2). Here, the $0.5\ \Omega$ sensing resistance R_s must be included in R. The product of these two gains is the overall feedback loop gain, which will vary simply as $1/\omega$ over the full frequency range, provided the two time constants are equal: $R_F C_F = L/R$, as in Figure 2. We approximately matched this condition for our x and y gradient coils with $L = 300\ \mu\text{H}$ and $R = 3\ \Omega$ (total), and $C_F = 4700\ \text{pF}$ and $R_F = 20\ \text{k}\Omega$. This matching is not critical.

Simple feedback theory suggests that a feedback loop gain $\propto 1/\omega$ and the associated 90° phase shift is the generally desired behavior. This situation results in a phase margin of 90° that protects against oscillation resulting from unforeseen phase shifts that can turn the feedback from negative to positive (when a total 180° is accumulated). Further, the output response to a step input voltage is an exponential rising or falling as $\exp(-\omega''t)$, where ω'' is the frequency where the loop gain has fallen to unity. One can generally push ω'' well above R/L without oscillation, meaning a faster exponential response to a step input, compared to running the same load in CV mode. For the values in Figure 2, ω'' is $2 \times 10^5 \text{ s}^{-1}$, corresponding to a closed loop time constant of $5 \mu\text{s}$, much faster than the CV time constant of $L/R=100 \mu\text{s}$. For a given product $R_F C_F$, the overall loop gain can be increased by increasing R_F (and decreasing C_F). The audio power amplifier also has a variable gain (A_v) that can be easily adjusted from the front panel to reduce the overall loop gain. However, if the power amplifier gain is reduced too much, the output from the current control circuit (U3, U4) will be unable to drive the power amplifier to the maximum gradient current required for a given experiment. It is important to note that, for a given set point voltage from the DAC, the value of A_v does not affect the resulting gradient current (at DC).

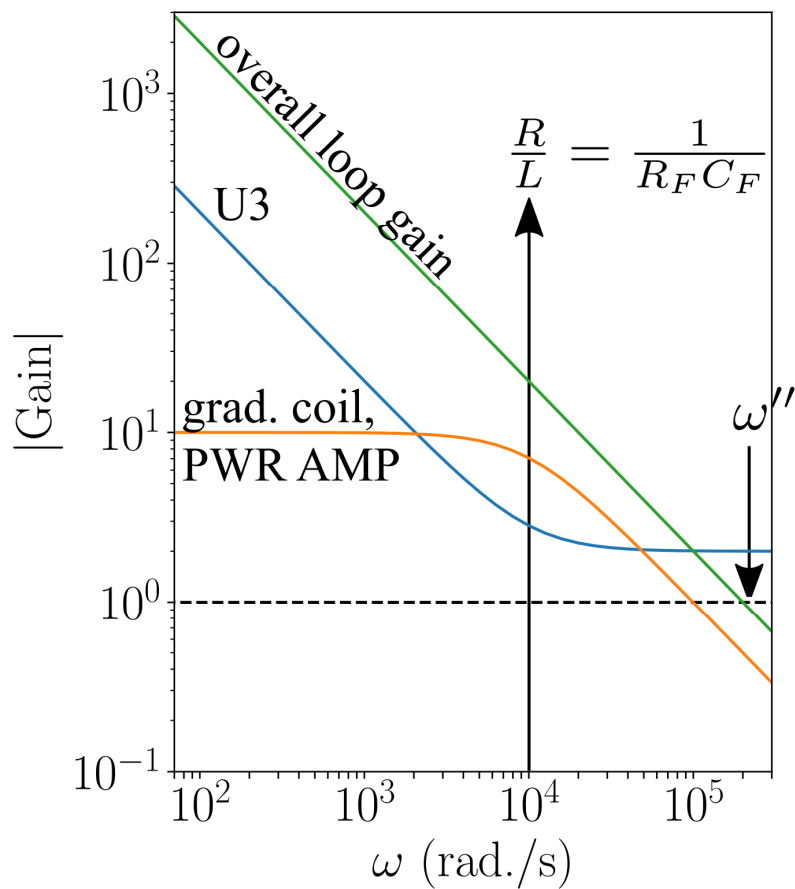


Figure 2: Feedback loop gain for CC operation. Blue: Gain of U3 with its associated feedback network. Orange: Gain from remaining components in the feedback loop involving the L/R time constant. The product of the orange and blue curves gives the overall loop gain (green), which falls below unity above ω'' .

The test of good $R_F C_F$ compensation is to look at the current waveform (using an oscilloscope) while driving the input with a trapezoidal waveform with, for example, 200 μ s ramps. Our CC front end has a monitor port and a rotary switch to allow monitoring of I_x , V_x , I_y ,... Excessive gain leads to ringing at sharp edges, a sign that self-oscillation (to be avoided) is near. In our hands and with our x and y gradient coils, the component values described for R_F and C_F work well; there is no suggestion of oscillation with the Samson Servo 600 at full gain and the current output is a faithful copy of the input trapezoid. On an oscilloscope the input and output traces are essentially identical. The z channel oscillates at a high frequency at full gain, so the gain is reduced for that channel; we believe the lower inductance L (85 μ H) of that simpler gradient coil is the reason.

The CC front end is powered by a wall transformer and has +15 V and -15 V 3-pin regulators. Lots of decoupling capacitors (twelve 0.22 μ F ceramic and six 22 μ F electrolytic) are used, as good practice. The circuitry is built on perforated board (it could be reduced to a small printed board) and mounted in an aluminum chassis. The feedback components R_F and C_F are mounted on 14-DIP carriers, plugged into 14-DIP sockets, to allow these components to be changed for different gradient coils. Standard TRS audio connectors with shielded balanced twisted pairs are used to connect to the DAC and from the CC chassis to the audio amplifiers. The three amplifier outputs go to an output box with suitable connectors mating to our gradient coils. The high sides of the outputs are fused in the output box, to protect the amplifiers and (crucially) the gradient coils. We use standard-speed 5 A cartridge fuses and have never had one blow. The inputs to U1 and U2 within the CC chassis (from the DAC connectors and from the current sensing resistors) are delivered by twisted pairs, to avoid inductive power-line pick-up. The current sensing 50 W power resistors R_s are thermally sunk to the chassis and a large aluminum slab. These are relatively low temperature coefficient units (± 50 ppm/C), as the fidelity of the gradient current I relies on the constancy of R_s , through the null balance equation $I R_s = V_{DAC}$.

RESULTS

The system of 3 channels, with two Samson Servo 600 amplifiers and the CC front end, costs about \$1200. The two Samsons (each with two channels) are about \$700 of this. If one started with Crown amplifiers modified by AE Techron, the cost would be about \$2500. We have used the CC-driven Samson amplifiers in our 11.35 MHz imager, based on a large-gap (10 cm) permanent magnet. 2D and 3D images of a hexagonal array of plastic tubes filled with water (see single slice shown in Figure 3) were indistinguishable from images made with a set of three AE Techron 2105 amplifiers (not shown). Room temperature drift causes the B_0 value to drift slowly; we interrupt the imaging sequence and automatically reset the frequency every four minutes to correct for this.

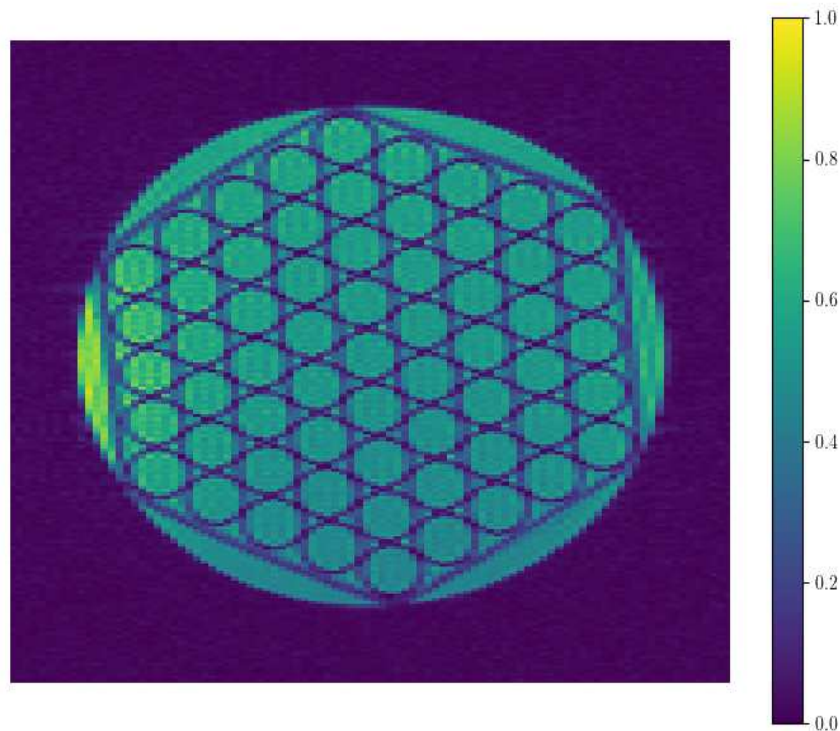


Figure 3: A 0.5 mm slice from a 3D image of a phantom (array of 5 mm OD plastic tubes immersed in water).

CONCLUSIONS

Audio power amplifiers can be modified to achieve DC coupling and become the basis of inexpensive gradient amplifiers, suitable for small NMR imaging systems. Instructions for modifying a Samson product are presented (see Appendix); a commercial alternative is Crown amplifiers modified by AE Techron. The amplifiers can directly drive small gradient coils in constant voltage (CV) mode. A simple constant current (CC) circuit in front of the audio amplifiers, as described herein, will result in true CC operation. The performance is excellent provided the amplifiers' limits are not exceeded.

APPENDIX: Conversion of Samson Servo 600 to DC coupling

This Samson amplifier was selected because it is an analog (not switching) design, the power output level is right for our needs, the circuit diagram is available [11], and the printed board is clearly marked (silk screened) and is not multilayer (so, easy to work on). Lower output power versions are available, too: the Samson Servo 300 and 200. Importantly, one side of the output of this amplifier (and many others) is essentially at ground, so U2 in the CC circuit does

not need to handle excessive common-mode voltages. Some amplifiers have a push-pull design in which neither output terminal is near ground. We note that the “bridged mode” of the Samson amplifiers for obtaining yet higher output voltages, is such a push-pull arrangement. To provide a stabilizing feedback loop to such an amplifier, current sensing would need to be implemented differently. “High-side” differential amplifiers with the ability to handle large common mode voltages could be used. Other options include the use of a DC-DC transformer or careful placement of the sense resistor near a low voltage point in the circuit (for instance, near the electrical center of the gradient coil). We choose to avoid the bridged-mode of our Samson Servo 600.

This unit has two input amplifier boards and two power output modules. On each power output module, one must short capacitors C9 and C10 using small insulated wires. Here it is best to work from the top of the board, since removing the board would entail lifting the six power transistors from the heat sink. All the boards are labelled (“silk screened”), making it easy to find the components. On the CH1 input board, short capacitors C2, 5, 7, 13, 22, 26, 27, 29, 30, and 32; we like to simply run a bead of solder across the two terminals on the solder side of the PC board. On the CH2 input board, short capacitors C14, 15, 33, 35, and 37. For this work, the power modules and input boards are loosened from the chassis, but the connecting wiring is left mostly intact. The three power leads (at a 3-pin connector with red, white, and black wires) and the red output lead for each power module (a blade and scabbard connector) are removed, as are the small, 2-pin signal input connectors for the power modules with white and black wires. The wiring to/from the input boards is left alone. A circuit diagram for the Servo 600 is available. While we have never used the smaller versions (Servo 300 and 200), the circuits are essentially identical.

Acknowledgements

We acknowledge the support of the Natural Sciences and Engineering Research Council of Canada (NSERC). We acknowledge funding by a subcontract from Texas A&M AgriLife, for ARPA-E grant ROOTS . The authors have no competing financial interests in the device or products described herein.

The information, data, or work presented herein was funded in part by the Advanced Research Projects Agency-Energy (ARPA-E), US Dept of Energy, under award number DE-AR0000823. The views and opinions of authors expressed herein do not necessarily state or reflect those of the US government or any agency thereof.

References

- [1] M. Kumar, L. Huber, H. Huang, Z. Shen and H. Jin, "Balancing control of paralleled full-bridge converters in high-current gradient amplifiers for MRI applications," *2020 IEEE Applied Power Electronics Conference and Exposition (APEC)*, 1222-1229, 2020.
- [2] J. A. Sabaté, R. R. Wang, F. Tao and S. Chi, "Magnetic Resonance Imaging Power: High-Performance MVA Gradient Drivers", *IEEE Journal of Emerging and Selected Topics in Power Electronics*, 4, 1, 280-292, 2016.
- [3] S. Li, B. Cao, D. Bi and X. Jiang, "Stacked high/low voltage level H-bridge circuit for gradient amplifier of MRI system", *2008 International Conference on Electrical Machines and Systems*, 2154-2158. 2008.
- [4] T. O. Reilly and A. G. Webb, "In vivo 3D brain and extremity MRI at 50 mT using a permanent magnet Halbach array," *Magnetic Resonance in Medicine*, 85, 495– 505, 2020.
- [5] C. Z. Cooley *et al.*, "Design and implementation of a low-cost, tabletop MRI scanner for education and research prototyping," *Journal of Magnetic Resonance*, 310, 106625, 2020.
- [6] S. M. Wright *et al.*, "A desktop magnetic resonance imaging system," *Magnetic Resonance Materials in Physics, Biology and Medicine*, 3, 177-185, 2002.
- [7] M. Meixner, J. Kochs, P. Foerst, and C. W. Windt, "An integrated magnetic resonance plant imager for mobile use in greenhouse and field," *Journal of Magnetic Resonance*, 323, 106879, 2021.
- [8] G.C. do Nascimento, R.E. de Souza, and M. Engelsberg, "A simple, ultralow magnetic field NMR imaging system", *Journal of Physics E: Scientific Instruments*, 22, 774-779 (1989).
- [9] G. C. Bagnall *et al.*, "Low-field magnetic resonance imaging of roots in intact clayey and silty soils," *Geoderma*, 370, 114356, 2020.
- [10] AE Techron. <https://aetechron.com>
- [11] Samson Servo 600 circuit diagram. Accessed Online <https://www.audioservicemanuals.com/s/samson-audio/samson-audio-servo200/>

